Int. J. Heat Mass Transfer. Vol. 35, No. 10, pp. 2421–2428, 1992
Printed in Great Britain

0017-9310/92 $5.00+0.00
Pergamon Press Ltd

Local heat transfer in a vertical gas-cooled tube with turbulent mixed convection and different heat fluxes

J. V. VILEMAS, P. S. POŠKAS and V. E. KAUPAS

Institute for Physical and Engineering Problems of Energy Research, Lithuanian Academy of Science, Kaunas, Lithuania

(*Received* 22 *January* 1991)

Abstract—The results of an experimental investigation of the local heat transfer in a vertical gas(air)-cooled tube with mixed turbulent convection under the conditions of codirected forced and free convection at $Re_{in} = (0.3\text{–}5) \times 10^4$, buoyancy parameter $K_{in} = (0.8\text{–}337) \times 10^{-5}$ and heat flux parameter $q_{in}^+ = (0.35\text{–}2.4) \times 10^{-3}$ are reported. An analysis of local heat transfer along the tube length is performed at different degrees of the effect of buoyancy forces and different heat fluxes. Characteristic regimes of heat transfer with a monotonous variation of the wall temperature and with non-uniform wall temperatures along the tube length are revealed. Correlations are obtained for calculating local heat transfer along the tube in the case of weak and strong effect of buoyancy forces. To obtain correlations for the intermediate region of the effect of buoyancy forces, further investigations are required.

1. INTRODUCTION

IT IS A frequent occurrence in heat exchanging equipment that the process of heat transfer is accomplished by combined connection, i.e. heat is simultaneously transferred due to a forced flow of a coolant and due to natural convection. For this reason, investigation of heat transfer under such conditions is of great interest, especially under a supercritical pressure of coolants. The latest review of studies of heat transfer in vertical tubes is presented in ref. [1]. In the case of a turbulent flow in vertical tubes with oppositely directed forced and free convections, the heat transfer rate increases under the influence of buoyancy forces, whereas with coinciding directions of convections, this rate first decreases, but then, with a further increase in the effect of free convection, it begins to increase. Moreover, when the directions of forced and natural convection coincide, characteristic maxima of the wall temperature appear along the tube length. These were observed for the first time by Shitsman in his studies of heat transfer under the conditions of supercritical pressures of a coolant [2]. Later, such local wall temperature maxima were discovered in ref. [3] at a water pressure of 5 bar and in ref. [4] at the atmospheric pressure of water.

In the case of gas coolant flows with codirected forced and natural convections, one also observes the general laminarizing effect of buoyancy forces [5–12]; however, there is a distinct lack of systematic data on the behaviour of local wall temperature maxima. In these works emphasis was given to the study of heat transfer far from the start of heating, in the region of the so-called stabilized heat transfer. Greater attention to the analysis of heat transfer along the tube length was paid in refs. [6, 8, 12], however in these works the data were obtained for short tubes, $x/d \leqslant 65$, and over a limited range of the effect of buoyancy forces.

The present paper reports experimental data on local heat transfer with mixed convection in a long ($x/d = 110$) vertical tube with codirected forced and natural convections in the cases of different heat fluxes over a wide range of operational parameters ($Re_{in} = (0.3\text{–}5) \times 10^4$, $K_{in} = (0.8\text{–}337) \times 10^{-5}$, $q_{in}^+ = (0.35\text{–}2.4) \times 10^{-9}$). The experimental study of the processes of heat transfer under these conditions, especially in the presence of local drops and rises in the heat transfer rates, is of great theoretical and practical importance, since numerical investigations cannot as yet produce sufficiently reliable results [1].

2. EXPERIMENTAL PROCEDURE

Investigations were carried out in an open-type wind tunnel. Under a pressure of 200 bar, the air, cleaned of impurities and moisture, was directed from a compressor station to high-pressure chambers and thence, through a reducer and pressure regulator, to a low-pressure receiver (under 8 bar), therefrom, through one of the three parallel lines with matched orifice plates of different clear areas, the air was supplied to the test section after which it was vented to the atmosphere through a throttle valve. The air flow rate was determined from the pressure difference on the orifice plates, from the static pressure and temperature of air ahead of the orifice plates. At small air flow rates (1–25 kg^{-1}), a flowmeter was used. Its main element is a nozzle at the exit from which a uniform velocity profile developed. The air flow rate was determined from the measured dynamic head and tem-

NOMENCLATURE

d	tube diameter [m]
g	free fall acceleration [m s^{-2}]
Gr	Grashof number, $g\beta q_w d^4/\lambda\nu^2$
Gr_A	Grashof number based on temperature gradient, $Gr/4Re\,Pr$
i	enthalpy [J kg^{-1}]
K	thermogravitational parameter, Gr_A/Re^2
Nu	Nusselt number
Pr	Prandtl number
q	specific heat flux [W m^{-2}]
q^+	heat flux parameter, $q_w/iu\rho$
Re	Reynolds number
u	mean mass velocity [m s^{-1}]
x	distance from the start of heating [m].

Greek symbols

β	coefficient of volumetric expansion [K^{-1}]
λ	thermal conductivity [W m^{-1} K^{-1}]
ν	kinematic viscosity [m^2 s^{-1}]
ρ	density [kg m^{-3}].

Subscripts

in	at the inlet to heat transfer section
T	forced turbulent convection heat transfer
w	wall
∞	over stabilization section.

perature in the inlet section of the nozzle. The flow temperature ahead of the orifice plates and in the flowmeter was measured using chromel–alumel thermocouples made of a 0.3 mm diameter wire; the static and dynamic pressures were measured by HBM PDI pressure transducers.

The main element of the test section was a 6950 mm long calorimetric tube made of type 1X18H1OT stainless steel with an outer diameter of 38.5 mm and wall thickness of 1.1 mm. The lower part of the tube 2500 mm long served as a section of hydrodynamic stabilization while the upper part 4295 mm long was heated by a constant electric current. The current was regulated by changing the voltage impressed on the excitation winding of the transformer and was determined from its drop across the shunt. The high stability of the generated current, and thus of heat release, was achieved by a special electronic regulator with a negative feedback.

To diminish heat losses into the surroundings, the calorimetrically studied portion of the tube was placed into a vacuum chamber, whereas its heated part was surrounded by eight cylindrical reflecting screens made of 0.2 mm thick polished sheet stainless steel. The body of the vacuum chamber also served as the load-carrying structure for the test section.

In order to stabilize the emissivity, the calorimetric tube was subjected to a preliminary two-hour burning in air at the wall temperature $T_w = 1090$ K. At 70 cross sections on opposite sides of the outer surface of the calorimetric tube there were resistance-welded chromel–alumel thermocouples. They were fabricated from a 0.3 mm diameter wire coated with heat-resistant insulation and were used for measuring both the wall temperature and voltage drop along the tube. To determine heat losses into the surroundings, 16 thermocouples were located along the first reflecting screen.

The air pressure, which varied from the atmospheric 1 to 8 bar, was measured at the test section inlet. A more detailed description of the test section is given elsewhere [13].

All the electrical signals from thermocouples and pressure transducers, as well as voltage drops across the calorimetric tube and shunt were measured with the aid of an automatic measuring system.

In processing the data, variations in geometric dimensions due to thermal expansion, heat losses through the vacuum-screen insulation, streamwise heat overruns in the tube wall and temperature drops across the wall were taken into account. The investigations were carried out at the boundary condition close to q_w = constant.

To increase the accuracy of determination of heat losses through the vacuum-screen insulation, special calibration tests were carried out. For this purpose, the tube clear area was filled with electric- and heat insulating material (asbestos cord) to prevent heat removal by natural convection. At a certain amount of electrical heating of the tube, the heat flux through the insulation was determined depending on the temperature difference between the tube walls and the screen.

The entrance to the calorimetric tube was made smooth with the profile evolving to Vitoshinskiy shape and therefore the transition of laminar flow to turbulence under isothermal conditions started at $Re_{cr1} \simeq 3000$ and ended at $Re_{cr2} \simeq 4500$, as evidenced by the measurements of the intermittency coefficient of streamwise velocity fluctuations.

When analyzing and correlating the data in terms of similarity numbers, the determining parameters were taken to be the inner diameter of the tube, pressure and temperature of air the test section inlet (labelled 'in') or local mean mass flow temperature in the section analyzed (x/d).

3. RESULTS OF EXPERIMENTAL INVESTIGATION

Investigation of heat transfer at atmospheric air pressure on the set-up described above showed [13] that under these conditions the heat transfer rate is close to that observed in the case of purely forced

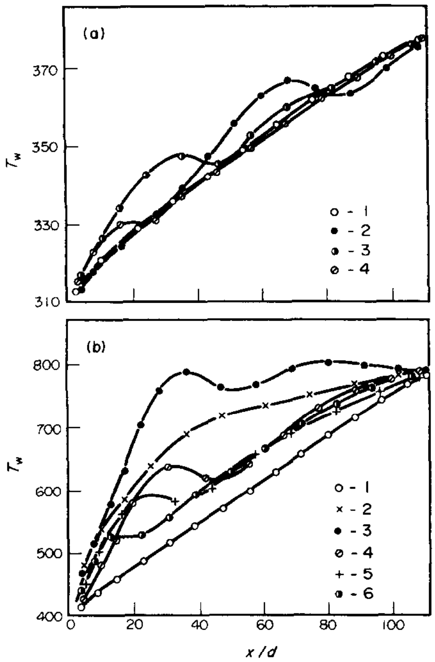

FIG. 1. Wall temperature variation along the tube length with coinciding forced and natural convections. (a) $q^+_{in} \simeq 0.000\,35$ and (1) $Re_{in} = 1.45 \times 10^4$, (2) 1.24×10^4, (3) 8.85×10^9, (4) 5×10^9. (b) $q^+_{in} \simeq 0.002\,36$ and (1) $Re_{in} = 5.29 \times 10^4$, (2) 3.23×10^4, (3) 2.48×10^4, (4) 2.07×10^4, (5) 1.64×10^4, (6) 1.14×10^4.

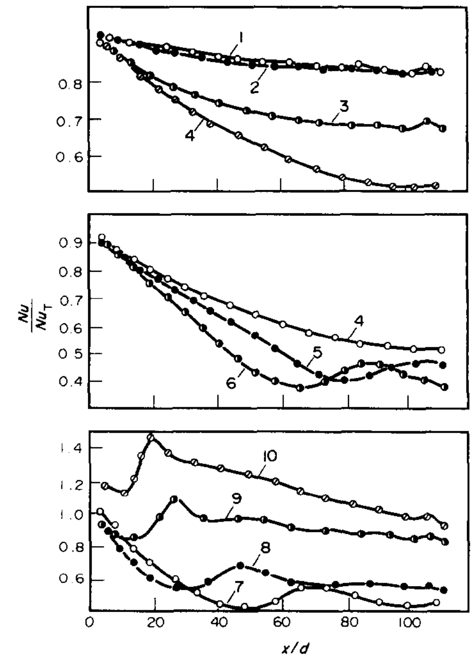

FIG. 2. Variation in the relative heat transfer rate along the tube length at $q^+_{in} \simeq 0.000\,35$. (1) $Re_{in} = 2.42 \times 10^4$, $K_{in} = 1.38 \times 10^{-5}$, (2) 1.94×10^4, 2.21×10^{-5}, (3) 1.61×10^4, 3.14×10^{-5}, (4) 1.45×10^4, 3.58×10^{-5}, (5) 1.33×10^4, 3.63×10^{-5}, (6) 1.24×10^4, 3.79×10^{-5}, (7) 1.14×10^4, 4.85×10^{-5}, (8) 8.85×10^9, 9.47×10^{-5}, (9) 5×10^9, 36.8×10^{-5}, (10) 3.7×10^9, 7×10^{-5}, Nu_T as in ref. [14].

convection. At elevated air pressure the process of heat transfer varies drastically and the effect of buoyancy forces starts to show up, so mixed convection heat transfer takes place. It is shown in Fig. 1 how the tube wall temperature varies at different values of Re_{in} when air pressure is $p = 7$ bar and the heat flux is variable. It is seen that in the case of coinciding forced and natural convections along the tube length and with a gaseous coolant, characteristic non-uniformities in the wall temperature appear that become more and more pronounced at increased heat fluxes (Fig. 1(b)). Although the wall temperature non-uniformity along the tube length at small heat fluxes is slight, the degree of heat transfer non-uniformity along the tube length turned out to be very appreciable under certain operating conditions when heat fluxes along the tube wall are correctly taken into account.

Figure 2 shows the change in the relative Nu along the tube length at different effects of buoyancy forces in the case of lowest heat flux. When the effect of buoyancy forces along the entire tube length is weak, the heat transfer rate decreases due to flow laminarization. At the beginning of the heated section it corresponds to forced convection heat transfer, whereas at the end of the tube the heat transfer rate is at a minimum (Fig. 2, curves 1 and 2). As the effect of buoyancy forces increases, the heat transfer rate begins to change more sharply, but in this case too its minimum is located at the end of the tube (Fig. 2, curves 3 and 4). With a further increase in the effect of buoyancy forces, the heat transfer rate over the initial thermal length continues to decrease gradually, but at certain distances from the start of heating its local maxima appear subsequent to which a decrease is again observed (Fig. 2, curves 5 and 6). The greatest decrease in the heat transfer rate is observed precisely in the regimes of the first manifestations of local heat transfer non-uniformities along the tube length (Fig. 2, curve 6). With a further increase in the effect of buoyancy forces the heat transfer minima (maxima) begin to shift to the side of the inlet cross-section, whereas generally its decrease slows down. This tendency of the shift of heat transfer minima (maxima) is also preserved at greater values of K_{in} (Fig. 2, curves 7–10), with the periodicity of its variation being more clearly expressed.

At elevated heat fluxes the process of mixed convection heat transfer is somewhat different. Let us analyze the relative heat transfer at $q^+_{in} \simeq 0.001\,27$ in more detail (Fig. 3). In the case of a small effect of buoyancy forces, the heat transfer rate along the tube length decreases little with distance from the start of heating (Fig. 3, curve 1), as was the case with constant physical properties of a coolant (Fig. 2). As the effect of buoyancy forces increases, the heat transfer rate keeps decreasing, but the significant fact is that its minimum is no longer located at the end of the tube, but somewhere in the middle of it (Fig. 3, curve 2). With a further increase in the effect of buoyancy forces

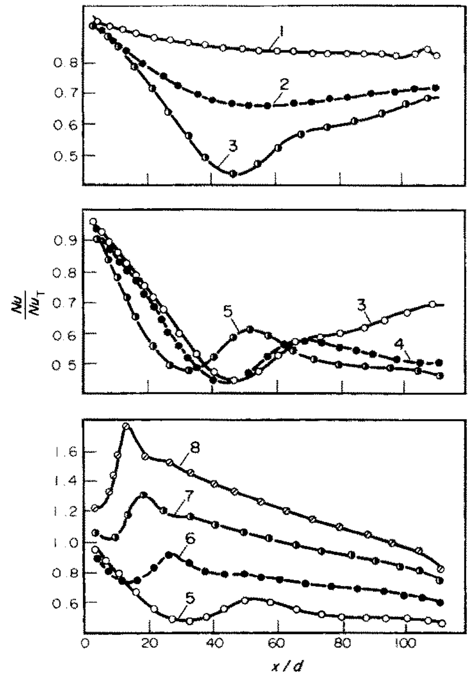

FIG. 3. Variation in the relative heat transfer rate along the tube length at $q_{in}^+ \simeq 0.00127$. (1) $Re_{in} = 3.33\times10^4$, $K_{in} = 2.28\times10^{-5}$, (2) 2.41×10^4, 4.58×10^{-5}, (3) 2.14×10^4, 5.52×10^{-5}, (4) 1.96×10^4, 5.71×10^{-5}, (5) 1.68×10^4, 8.06×10^{-5}, (6) 9.55×10^9, 29.8×10^{-5}, (7) 6.16×10^9, 88×10^{-5}, (8) 4.54×10^9, 181×10^{-5}, Nu_T according to ref. [14].

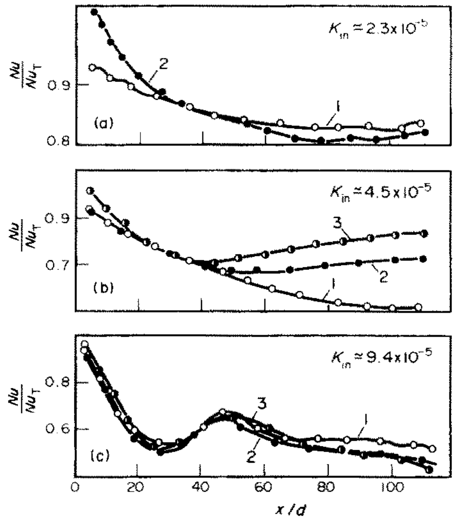

FIG. 4. Comparison of the relative heat transfer rate at different heat fluxes. (1) $q_{in}^+ \simeq 0.00035$, (2) 0.00127, (3) 0.00236, Nu_T according to ref. [14].

the bend in the heat transfer curve (Fig. 3, curve 3) degenerates into a local maximum of heat transfer (Fig. 3, curve 4). Afterwards the regimes with specific minima and maxima (Fig. 3, curves 5–8) appear which also took place in the case of the constant physical properties of the coolant (Fig. 2). As the buoyancy parameter grows, these minima (maxima) also shift to the side of the flow inlet (Fig. 3, curves 5–8). At a higher heat flux, large values of the buoyancy parameter are attained, whereas the point of the first minimum of heat transfer rate is located near the start of heating (Fig. 3, curves 7 and 8), i.e. the zone of turbulent boundary layer laminarization virtually disappears, and the heat transfer rate begins to increase immediately with x/d. Having reached a certain maximum, however, it begins to decrease, as was the case in the previous regimes.

With a further increase in the heat flux, the qualitative behaviour of heat transfer varies little. There are the same regimes with a minimum of heat transfer rate (without its local maximum), with a characteristic bend and with the minima and maxima of heat transfer rate. Henceforth, they go over into the regimes with the maximum of heat transfer rate when the point of its minimum has already been shifted to the start of heating.

In Fig. 4 the data on the relative heat transfer rate at $K_{in} = \text{idem}$ but at different values of q_{in}^+ are compared. It is seen that with the data being represented in this fashion, the relative local heat transfer rate in the case of a weak effect of natural convection is virtually independent of the magnitude of heat flux q_{in}^+ (Fig. 4(a)), i.e. the effect of the change in the physical properties of the gas is rather well taken into account by the parameter K_{in} and by the number Nu_T calculated for the forced coolant flow with account for this change. With a strong effect of free convection, the magnitude and location of characteristic minima and maxima of heat transfer rate are also independent of the heat flux magnitude (Fig. 4(c)). Downstream of the maximum, however, the heat transfer rate begins to depend to some extent on q_{in}^+. The greatest effect of q_{in}^+ is observed in the case of moderate effect of natural convection (Fig. 4(b)).

To calculate the heat transfer rate far from the start of heating ($x/d > 40$) in the natural convection mode the following relation was suggested [11]:

$$St_{NC} = E^{1/4}[1.33\lg(Re/8)+3.3(Pr^{2/3}-0.7)]^{-1} \quad (1)$$

where $E = Gr_q/(Re^4\ Pr)$. It is also shown there that with $E < 5\times10^{-7}$ the experimental points obtained by various authors for mixed convection deflect downwards from this relation, i.e. at such values of E the heat transfer rate (the value of St) is smaller than it would have been in the natural convection mode.

In the experiments carried out by the present authors the parameter E in a turbulent flow at the inlet was also below this limit (i.e. $E < 5\times10^{-7}$), therefore, as is seen from Fig. 5, the heat transfer rate at large values of x/d is smaller than in the case of natural convection (St_{NC}). Of interest is the fact that at the points of local maximum the heat transfer rate at both constant (Fig. 5(a)) and variable (Fig. 5(b)) properties of air is close to such under conditions of natural convection. Consequently, the pattern of flow and heat transfer typical of the natural convection regime is first of all achieved at the points of the heat transfer rate extrema.

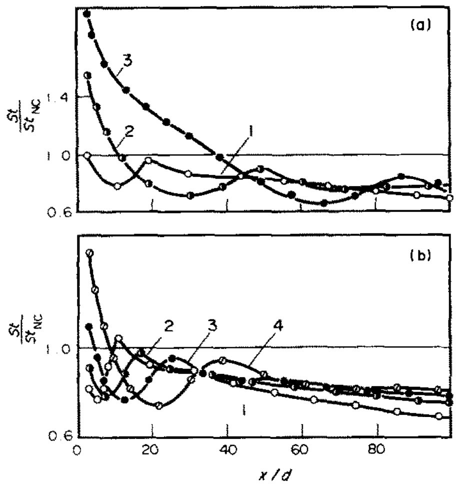

FIG. 5. Comparison of heat transfer for mixed and natural convection (St and St_{NC}). (a) $q^+_{in} \simeq 0.000\,35$, (1) $Re_{in} = 3.7\times10^9$, $E = 8\times10^{-7}$–5.4×10^{-7} (the first value corresponds to $x/d \simeq 3$, the second value to $x/d \simeq 100$, (2) 8.85×10^9, 4.2×10^{-8}–3.2×10^{-8}, (3) 1.24×10^4, 1.26×10^{-8}–0.97×10^{-8}, (b) $q^+_{in} \simeq 0.002\,36$, (1) $Re_{in} = 4.64\times10^9$, $E = 25.5\times10^{-7}$–3.65×10^{-7}, (2) 7.82×10^9, 4.66×10^{-7}–0.88×10^{-7}, (3) 1.14×10^4, 12.1×10^{-8}–2.96×10^{-8}, (4) 1.64×10^4, 3.37×10^{-8}–8.42×10^{-9}.

On the practical side, it is important to know the limits between characteristic groups of mixed convection heat transfer regimes. The schematic representation of their division is given in Fig. 6.

When $K_{in} < K_{in1}$, the effect of free convection on forced heat transfer can be neglected. The value of K_{in1} ($K_{in1} = (2$–$4)\times10^{-6}$) was determined using the recommendations [11] for the limited Grashof number at constant physical properties of the coolant, however, as mentioned earlier, if there is a weak effect of natural convection, the relative heat transfer rate is independent of q^+_{in}, and therefore it was assumed that K_{in1} would also not depend on the variability of the physical properties of the coolant.

When $K_{in1} < K_{in} < K_{in2}$, there is a region of weak effect of free convection. In this region, the relative heat transfer rate decreases uniformly along the tube length and is independent of the heat flux magnitude. The value of K_{in2} is, therefore, also independent of the heat flux magnitude and is equal to 2.5×10^{-5}.

The intermediate region spans over the range $K_{in2} < K_{in} < K_{in3}$ and its width depends on heat flux. To determine K_{in3}, the following relation is suggested

$$K_{in3} = 1.5\times10^{-3}(q^+_{in})^{0.45}. \qquad (2)$$

In the intermediate region the uniform heat transfer rate distribution transforms into a non-uniform one with characteristic minima and maxima. Here, as the heat flux increases, there appear regimes with a characteristic minimum of heat transfer rate as well as regimes with a characteristic bend.

When $K_{in} > K_{in3}$, the natural convection exerts a strong influence on the process of heat transfer, and there are regimes with minima and maxima (or only with the maximum) of heat transfer rate irrespective of the heat flux magnitude.

4. CORRELATION OF TURBULENT FLOW RESULTS

To calculate the mixed turbulent convection heat transfer in vertical tubes with coinciding directions of

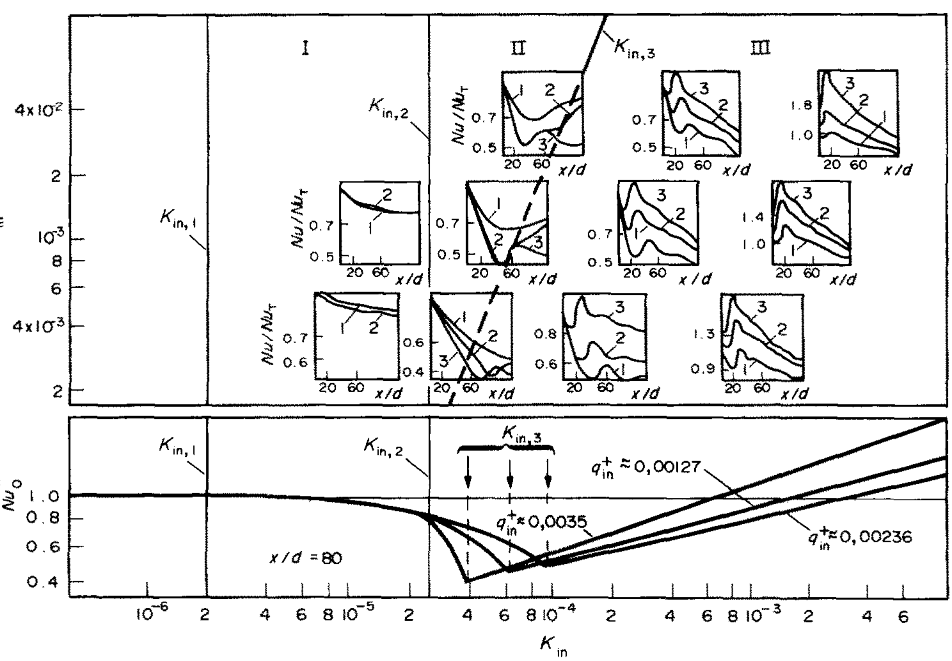

FIG. 6. Schematic representation of the effect of buoyancy forces on the process of heat transfer at different heat fluxes. I, region of weak effect of natural convection; II, intermediate region; III, region of strong effect of natural convection.

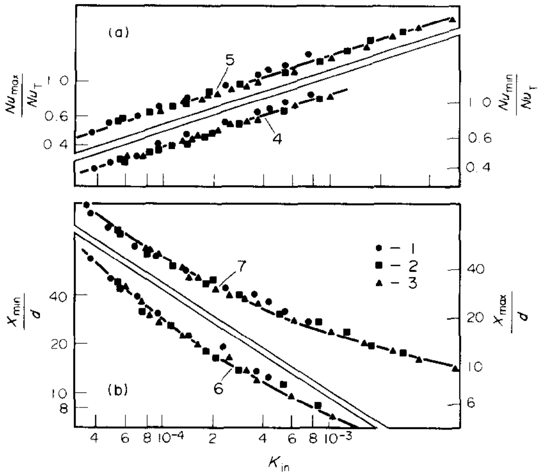

FIG. 7. Relative heat transfer rate (a) at the point of its local maximum (Nu_{max}) and minimum (Nu_{min}) and the location of the extremal points of heat transfer rate (b): local maximum (x_{max}/d) and minimum (x_{min}/d) at different heat fluxes q^+_{in}. (1) $q^+_{in} \simeq 0.000\,35$, (2) 0.001 27, (3) 0.002 36, (4)–(7) from relations (4)–(7), respectively. Nu_T according to ref. [14].

forced and natural convections, a number of correlations have been suggested [1, 11]. They are, however, suited to application only in the so-called region of stabilized heat transfer. Only one work [15] is known at present which suggests a procedure for calculating the local heat transfer rate in a water flow through a tube. To describe the local heat transfer rate in the regimes with the minima and maxima of wall temperature, the following relation is used which gives a decaying cosine curve

$$\frac{Nu}{Nu_T} = \left(\frac{Nu}{Nu_T}\right)_\infty + A\cos\left\{\pi\left[\left(\frac{x-x_{min}}{d}\times\frac{T}{2}\right)-1\right]\right\} \tag{3}$$

where $(Nu/Nu_T)_\infty$ is the stabilized heat transfer; A and T are the amplitude and the period of the cosine curve; x and x_{min} are the distances from the start of heating to the calculated cross-section and to the first local minimum of heat transfer rate.

An attempt to correlate the present authors' data for an air flow by the technique suggested in ref. [15] has not been successful. For such regimes (the zone of strong effect of free convection (Fig. 6)) the technique used in the present work employs the heat transfer rate at the points of its local minimum and maximum and the distances to these points as the basic ones. When the quantity K_{in} is taken as the determining parameter (the physical properties of the coolant are determined from the inlet temperature), neither the relative heat transfer rate, nor the location of these points virtually depend on the heat flux magnitude (Fig. 7). The correlation of experimental data yielded the following relations:

$$Nu_{min}/Nu_T = 11.3K_{in}^{1/3} \quad \Delta = 8.9\% \quad \delta = 3.9\% \tag{4}$$

$$Nu_{max}/Nu_T = 14.5K_{in}^{1/3} \quad \Delta = 9.4\% \quad \delta = 5.4\% \tag{5}$$

$$x_{min}/d = 5.19+0.0059/K_{in}^{0.9} \quad \Delta = 9.7\% \quad \delta = 5.1\% \tag{6}$$

$$x_{max}/d = 8.8+0.063/K_{in}^{0.7} \quad \Delta = 10.3\% \quad \delta = 6\% \tag{7}$$

with corresponding maximum (Δ) and root-mean-square (δ) relative errors.

When correlating the data along the tube length in the zone with $K_{in} > K_{in3}$, the following division into three groups was made:

(1) the data for $0 < x/d < x_{min}/d$;
(2) the data for $x_{min}/d \leqslant x/d \leqslant x_{max}/d$;
(3) the data for $x/d > x_{max}/d$.

The data of the first group ($0 < x/d < x_{min}/d$) are correlated by the following relation:

$$\frac{Nu}{Nu_T} = \frac{Nu_{min}}{Nu_T} + (5.39\times10^{-9} + 5.12\times10^{-4}\ln K_{in})\left(\frac{x}{d}-\frac{x_{min}}{d}\right)^2$$

$$\Delta = 16\% \quad \delta = 5.1\% \tag{8}$$

the data of the second group ($x_{min}/d \leqslant x/d \leqslant x_{max}/d$) by the relation

$$\frac{Nu}{Nu_T} = \frac{Nu_{min}}{Nu_T} + (3.865\times10^{-9} + 3.672\times10^{-4}\ln K_{in})\left(\frac{x}{d}-\frac{x_{min}}{d}\right)$$

$$\Delta = 12\% \quad \delta = 4.3\% \tag{9}$$

and the data of the third group ($x/d > x_{max}/d$) by the relation

$$\frac{Nu}{Nu_T} = \frac{Nu_{max}}{Nu_T} - 3.555K_{in}^{0.92}\left(\frac{x}{d}-\frac{x_{max}}{d}\right)^{0.46}(q^+_{in})^{0.26}$$

$$\Delta = 9.4\% \quad \delta = 4.2\%. \tag{10}$$

As already mentioned, the heat transfer rate in the zone of the weak effect of free convection ($K_{in1} < K_{in} < K_{in2}$) is independent of the heat flux magnitude. The correlation of the data for this zone gave the relation

$$\frac{Nu}{Nu_T} = \frac{1}{0.98+0.54K_{in}^{0.25}(x/d)^{0.975}}$$

$$\Delta = 7.6\% \quad \delta = 3.3\%. \tag{11}$$

The heat transfer rate in the intermediate region ($K_{in2} < K_{in} < K_{in3}$) is very sensitive to the change in the buoyancy parameter K_{in} and in the heat flux magnitude and we failed to obtain correlations for calculating the local heat transfer rate in this region.

In ref. [9], a relation was suggested for calculating stabilized heat transfer in the case of coinciding forced

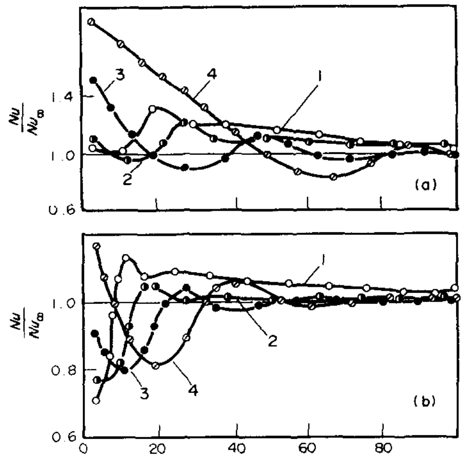

FIG. 8. Comparison of experimental data (Nu) with correlation (13) for stabilized heat transfer (Nu_∞), (a) $q_{in}^+ \simeq 0.00035$, (1) $Re_{in} = 3.7\times 10^9$, $K_{in} = 77\times 10^{-5}$, (2) $5\times 10^9, 36.8\times 10^{-5}$, (3) $8.85\times 10^9, 9.5\times 10^{-5}$, (4) 1.24×10^4, 3.8×10^{-5}, (b) $q_{in}^+ \simeq 0.00236$, (1) $Re_{in} = 4.64\times 10^9$, $K_{in} = 337\times 10^{-5}$, (2) 7.82×10^9, 103×10^{-5}, (3) 1.14×10^4, 38×10^{-5}, (4) 1.64×10^4, 14.5×10^{-5}.

and natural convections at different values of Pr

$$\frac{Nu_\infty}{Nu_T} = 8.84K^{0.263}. \qquad (12)$$

The analysis and generalization of the data of the present investigation for air flow at different heat fluxes have also yielded a relation with the same exponent at the buoyancy parameter $K = Gr_A/Re^2$, but with account for the effect of the heat flux magnitude q^+

$$\frac{Nu_\infty}{Nu_T} = 17K^{0.27}(q^+)^{0.1}. \qquad (13)$$

As is seen from Fig. 8, stabilization of heat transfer in regimes with wall temperature maxima is observed only at large values of x/d. The disregard of this fact may lead to substantial errors in determining the wall temperature in the initial section of the tube.

REFERENCES

1. J. D. Jackson, M. A. Cotton and B. P. Axell, Studies of mixed convection in vertical tubes, *Int. J. Heat Fluid Flow* **10**, 2–15 (1989).
2. M. Ye. Shitsman, Deteriorated heat transfer modes at postcritical pressures, *Teplofiz. Vysok. Temp.* **2**, 267–275 (1963).
3. D. B. R. Kenning, R. A. W. Shock and J. Y. Poon, Local reduction in heat transfer due to buoyancy effects in upward turbulent flow, *Proc. 5th Int. Heat Transfer Conf.*, Tokyo, Vol. 2, pp. 141–145 (1974).
4. N. M. Rouai, Influences of buoyancy and imposed flow transients on turbulent convective heat transfer in a tube, Ph.D. Thesis, University of Manchester (1987).
5. A. Mreiden, Etude de la structure de l'ecoulement et de transfer de chaleur en convection mixte dans un tube, These de Doct.-Ing., Faculte des Sci., Paris (1968).
6. A. Steiner, On the reverse transition of a turbulent flow under the action of buoyancy forces, *J. Fluid Mech.* **47**, 503–512 (1971).
7. J. E. Byrne and E. Ejiogu, Combined free and forced convection heat transfer in a vertical pipe, *Symposium Heat and Mass Transfer by Combined Forced and Natural Convection*, The Institution of Mechanical Engineers, Paper C 118/71, Manchester (1971).
8. J. A. Bates, R. A. Schmall, G. A. Hasen and D. M. McEligot, Effects of buoyant body forces on forced convection in heated laminarizing flows, *Proc. 5th Int. Heat Transfer Conf.*, Tokyo, Vol. 2, pp. 141–145 (1974).
9. M. A. Connor and A. D. Carr, Heat transfer in vertical tubes under conditions of mixed free and forced convection, *Proc. 6th Int. Heat Transfer Conf.*, Toronto, Vol. 1, pp. 43–48 (1978).
10. H. Tanaka, Sh. Maruyama and Sh. Hatano, Combined forced and natural convection heat transfer for upward flow in a uniformly heated vertical pipe, *Int. J. Heat Mass Transfer* **30**, 165–174 (1987).
11. B. S. Petikhov and A. F. Polyakov, *Mixed Turbulent Convection Heat Transfer*. Nauka, Moscow (1986).
12. A. F. Polyakov and S. A. Shindin, Development of turbulent heat transfer over the length of vertical tubes in the presence of mixed air convection, *Int. J. Heat Mass Transfer* **31**, 987–992 (1988).
13. J. Vilemas and P. Poškas, A study of heat transfer in vertical channels for high heat loads in the transition region, *Proc. Int. Heat Transfer Conf.*, San Francisco, Vol. 3, pp. 913–917 (1986).
14. B. S. Petikhov, V. A. Kurganov and A. I. Gladuntsov, *Heat and Mass Transfer*, Vol. 1, pp. 117–127. Izd. ITMO AN BSSR, Minsk (1972).
15. G. A. Kapinos and O. V. Remizov, *Teploenergetika* No. 2, 60–61 (1988).

TRANSFERT THERMIQUE LOCAL DANS UN TUBE VERTICAL REFROIDI PAR UN GAZ AVEC UNE CONVECTION TURBULENTE MIXTE ET DIFFERENTS FLUX THERMIQUES

Résumé—On donne les résultats d'une étude expérimentale du transfert thermique local dans un tube refroidi par un gaz (air) avec une convection thermique mixte turbulente, pour des conditions de convection forcée et naturelle dans le même sens, avec $Re_{in} = (0{,}3\text{–}5)\times 10^4$, paramètre de flottement $K_{in} = (0{,}8\text{–}337)\times 10^{-5}$ et paramètre de flux thermique $q_{in}^+ = (0{,}35\text{–}2{,}4)\times 10^{-3}$. Une analyse du transfert local thermique le long du tube est conduite pour différents degrés de l'effet des forces de flottement et différents flux thermiques. Des régimes caractéristiques de transfert de chaleur avec une variation monotone de la température pariétale et avec des températures pariétales non uniformes le long du tube sont révélés. Des formules sont obtenues pour calculer le transfert thermique local le long du tube dans le cas d'un effet faible ou fort des forces de flottement. Pour obtenir des formules relatives à la région intermédiaire de l'effet de flottement, d'autres recherches sont nécessaires.

ÖRTLICHER WÄRMEÜBERGANG IN EINEM SENKRECHTEN GASGEKÜHLTEN ROHR MIT TURBULENTER MISCHKONVEKTION UND UNTERSCHIEDLICHEN WÄRMESTROMDICHTEN

Zusammenfassung—Der örtliche Wärmeübergang in einem senkrechten gas (luft)-gekühlten Rohr mit turbulenter Mischkonvektion wird unter den Bedingungen einer gleichgerichteten erzwungenen und freien Konvektionsströmung für folgende Parameter untersucht: $Re_{in} = 0{,}3 \times 10^4$–$5 \times 10^4$; Auftriebsparameter $K_{in} = 0{,}8 \times 10^{-5}$–$337 \times 10^{-5}$; Wärmestromdichtenparameter $q_{in}^+ = 0{,}35 \times 10^{-9}$–$2.4 \times 10^{-9}$. Der örtliche Wärmeübergang entlang der Rohrlänge wird für unterschiedlich starken Einfluß der Auftriebskraft und für unterschiedliche Wärmestromdichten untersucht. Es werden charakteristische Bereiche des Wärmeübergangs für monotone Änderung der Wandtemperatur und für ungleichmäßige Verteilungen der Wandtemperatur entlang des Rohres aufgezeigt. Es ergeben sich Korrelationsgleichungen für den örtlichen Wärmeübergang entlang des Rohres für die Fälle schwacher und starker Beeinflussung durch Auftriebskräfte. Weitere Untersuchungen sind zur Beschreibung des Gebietes mittlerer Beeinflussung durch Auftriebskräfte erforderlich.

МЕСТНАЯ ТЕПЛООТДАЧА В ВЕРТИКАЛЬНОЙ ГАЗООХЛАЖДАЕМОЙ ТРУБЕ ПРИ ТУРБУЛЕНТНОЙ СМЕШАННОЙ КОНВЕКЦИИ И РАЗНЫХ ТЕПЛОВЫХ НАГРУЗКАХ

Аннотация—Представлены результаты экспериментального исследования местной теплоотдачи в вертикальной газоохлаждаемой (воздух) трубе при смешанной турбулентной конвекции в условиях совпадающих направлений вынужденной и свободной конвекций при $Re_{in} = (0{,}3$–$5) \times 10^4$, параметре термогравитации $K_{in} = (0{,}8$–$337) \times 10^{-5}$ и параметре теплового потока $q_{in}^+ = (0{,}35$–$2{,}4) \times 10^{-3}$. Проведен анализ местной теплоотдачи по длине трубы при различной степени воздействия термогравитационных сил и разной тепловой нагрузке. Выявлены характерные режимы теплоотдачи с монотонным изменением температуры стенки и с неравномерностями температуры стенки по длине трубы. Получены обобщающие зависимости для расчета местной теплоотдачи по длине трубы при слабом и сильном влиянии термогравитационных сил. Для получения обобщающих зависимостей в промежуточной области влияния термогравитационных сил необходимы дальнейшие исследования.